Computational Fluid Dynamics in 3D-Printed Scaffolds with Different Strand-Orientation in Perfusion Bioreactors

***Saatchi, Ali Reza*•**

School of Chemical Engineering, College of Engineering, University of Tehran, Tehran, I.R. IRAN

Seddiqi, Hadi

Department of Biomedical Engineering, Research Center for New Technologies in Life Science Engineering, University of Tehran, Tehran, I.R. IRAN

Amoabediny, Ghassem**+•

School of Chemical Engineering, College of Engineering, University of Tehran, Tehran, I.R. IRAN

Helder, Marco N.

Department Oral and Maxillofacial Surgery, VU University Medical Center/Academic Centre for Dentistry Amsterdam (ACTA), Amsterdam Movement Sciences, Amsterdam, THE NETHERLAND

Zandieh Doulabi, Behrouz; Klein Nulend, Jenneke

Department of Oral Cell Biology, Academic Centre for Dentistry Amsterdam (ACTA)-the University of Amsterdam and Vrije Universiteit Amsterdam, Amsterdam Movement Sciences, Amsterdam, THE NETHERLANDS

ABSTRACT: *Bone tissue engineering strategies use fluid flow dynamics inside 3D-scaffolds in perfusion, bioreactors mechanically stimulate cells in these scaffolds. Fluid flow dynamics depends on the bioreactor's inlet flow rate and 3D-scaffold architecture. We aimed to employ a computational evaluation to assess fluid dynamics in 3D-printed scaffolds with different angular orientations between strands in each layer inside a perfusion bioreactor at different inlet flow rates. 3D-printed cubic scaffolds (0.6×0.6×0.6 cm; total volume 216×10^{-3} cm^3) containing strands (diameter 100 µm) with regular internal structure and different angular orientation (30°, 45°, 60°, and 90° between strands in each layer) were used for modeling. The finite element method showed that the perfusion bioreactor's inlet flow rate (0.02, 0.1, 0.5 mL/min) was linearly related to average fluid velocity, average fluid shear stress, and average wall shear stress inside 3D-printed scaffolds with different angular orientation (30°, 45°, 60°, 90°) between strands in each layer. At all inlet flow rates, strands at 30° angular orientation increased average fluid velocity (1.2-1.5-fold), average fluid shear stress (6-10-fold), and average wall shear stress (1.4-2-fold) compared to strands at 45°, 60°, and 90° angular orientation providing similar results. In conclusion, significant local changes in fluid dynamics inside 3D-printed scaffolds result from varying the degree of angular orientation between strands in each layer, and the perfusion bioreactor's inlet flow rate. By decreasing the angular orientation between strands in each layer and increasing the inlet flow*

***** *To whom correspondence should be addressed.*

+ E-mail: amoabediny@ut.ac.ir

• Department of Biomedical Engineering, Research Center for New Technologies in Life Science Engineering, University of Tehran, Tehran, I.R. IRAN

1021-9986/2020/5/307-320 *14/$/6.04*

rate of a perfusion bioreactor, the magnitude and distribution of fluid velocity, fluid shear stress, and wall shear stress inside the scaffold increased. The average fluid velocity, average fluid shear stress, and average wall shear stress inside the scaffold within the bioreactor increased linearly with the inlet flow rate. This might have important implications for bone tissue engineering strategies using cells, scaffolds, and bioreactors.

KEYWORDS: *Bone tissue engineering; Fluid flow dynamics; Perfusion bioreactor; 3D-printed scaffold; Finite element modeling; Strand orientation.*

INTRODUCTION

A bone tissue-engineered construct has structural and mechanical characteristics that closely mimic natural bone tissue to allow successful clinical application. Dynamic bioreactors are used to overcome the drawbacks of static cultures, such as poor nutrient and waste exchange [1]. These bioreactors provide viable and homogeneous bone constructs with excellent osteogenic properties, thus providing an alternative for autologous grafts [2]. Although a clear relationship exists between mechanical loads, osteogenic differentiation of Mesenchymal Stem Cells (MSCs), and extracellular matrix mineralization [3], the assessment of local fluid dynamics sensed by cells inside 3D-scaffolds is almost impossible. Therefore, new methods are needed to assess local fluid dynamics inside dynamic bioreactors.

Dynamic bioreactor systems improve the quality of engineered bone tissue in 3-dimensions (3D) by allowing reproducible and controlled changes in specific biochemical and biomechanical factors. These systems allow rapid vascularization of bone constructs by stimulating proliferation and differentiation of endothelial progenitor cells, as well as vascularization of scaffolds implanted in vivo [4]. Perfusion systems enhance *in vitro* growth, differentiation [5], and mineralized matrix production [6]. Low perfusion flow rates (0.01-0.2 mL/min) increase osteoblast proliferation, while high rates (>1 mL/min) are associated with substantial cell death throughout a 3D-porous scaffold in a perfusion bioreactor [7]. Furthermore, perfusion fluid flow stimulates osteogenic differentiation of human MSCs, compared to static culture [3].

Fluid shear stress and mass transport modulate the fabrication of large-scale tissue engineered bone [3]. Mechanical stimulation by fluid shear stress is known to enhance bone tissue regeneration *in vitro* [8]. Osteocytes, the most sensitive bone cell type to mechanical stimulation, are also especially sensitive to fluid shear stress and transduce these mechanical stimuli into biochemical responses [9, 10]. Bone cells in vivo experience fluid shear stress from 800 to 3000 mPa in response to mechanical loading [11, 12]. Moreover, fluid shear stress determines lineage commitment [13]. It determines whether MSCs differentiate along the osteogenic or chondrogenic pathway [14]. Fluid shear stress stimulates osteogenic differentiation of bone marrow stromal, periosteum, and adipose-derived MSCs, and enhances extracellular matrix deposition [15]. Moreover, fluid shear stress can promote the efficiency of the differentiation protocols of adipose stem cells through independent mechanisms [16]. Therefore, quantification of flow-induced fluid shear stress within 3D-scaffolds in dynamic bioreactors is crucial for further development of bone tissue regeneration strategies in vitro.

Engineered 3D-scaffolds can overcome the limitations of autografting and allografting. Conventional 3D-scaffold fabrication techniques, e.g. material injections [17], solvent casting [18], phase separation [19], and freeze drying [20] do not precisely control the internal scaffold architecture or complex architecture fabrication. Scaffolds fabricated using these techniques have compressive moduli of maximally 0.4 MPa, i.e. much lower than compressive moduli of hard tissue (10–1500 MPa) [21]. Hence, rapid prototyping techniques, like 3D-printing, show improved design repeatability, part consistency, and control of scaffold architecture [22]. 3D-printing involves the laying down of successive layers of material to form 3D-models, thus enabling excellent control of pore size, pore morphology, and matrix porosity [23]. 3D-printed scaffolds can be produced at low cost, in a quick process, and have multimaterial capabilities which are useful for bone tissue engineering [22]. 3D-printing of scaffolds for bone tissue-engineering applications requires the fabrication

of highly porous scaffolds, which is achieved by fabrication of lay-down patterns of strands that are interconnected [24]. Scaffold architecture, e.g. angular orientation between strands inside 3D-printed scaffolds, influences osteogenic differentiation of pre-osteoblasts in perfusion culture [25].

Modeling and simulation of bone tissue-engineering systems are helpful to determine the effect of a 3D-scaffold architecture [25, 26] and bioreactor parameters (e.g. inlet flow rate [27]) on tissue engineered outcomes. Since the 3D-scaffold geometry is complex, it is difficult or even impossible when using experimental techniques to obtain biomechanical information inside the 3D-scaffolds and bioreactors. Mathematical modeling and simulation techniques of the fluid dynamics in the bone tissue growth process are helpful to investigate fluid flow dynamics and nutrient transport in complex porous tissue scaffolds inside perfusion bioreactors [28]. Simulation studies have shown that in circular scaffolds with a homogeneous geometry, the pore size (diameter 50 to 150 μm) influences the shear stress magnitude at the walls [29]. Furthermore, a flow rate of 0.04 mL/min leads to a surface area averaged wall shear stress of 1.41 mPa for titanium and 1.09 mPa for hydroxyapatite [30]. These studies show that input flow rate as well as scaffold architecture and porosity affect the wall shear stress on the scaffold surfaces. These simulations can be used to predict in vitro experimental and parametric study outcomes indicating which factors significantly affect the engineered output.

In the current study, we aimed to employ computational evaluation to assess fluid dynamics in 3D-printed cubic scaffolds (0.6×0.6×0.6 cm) containing strands of 100 μm diameter with different angular orientation between the strands in each layer inside a perfusion bioreactor with different inlet flow rates using a numerical (finite element) method. Varying angular orientation (30°, 45°, 60°, and 90° between strands in each layer) inside the 3D-printed scaffold and inlet flow rate (0.02, 0.1, and 0.5 mL/min) of a perfusion bioreactor, as controllable parameters, were used to simulate magnitude and distribution of fluid velocity, fluid shear stress, and wall shear stress within the 3D-printed scaffolds in perfusion bioreactors.

THEORETICAL SECTION

Design of scaffolds

3D-printed cubic scaffolds (0.6×0.6×0.6 cm; total volume 216×10^{-3} cm^3) containing strands (diameter 100 μm) with regular internal structure and different angular orientation (30°, 45°, 60°, and 90° between strands in each layer) were designed by COMSOL Multiphysics (v5.2). The size, shape, and distribution of the void channels inside the scaffolds were regular, and the channels were interconnected. The strands inside the scaffolds were assumed as solid, i.e. incompressible and impermeable for fluid, and the strands topography was considered constant during the computational evaluation. A schematic of the side view and top view of the scaffolds with strands used for the simulation is shown in Fig. 1. Since the scaffolds were considered as solid material, the physico-chemical composition of the scaffolds was undefined.

Perfusion bioreactor configuration

The inlet fluid was flowing homogenously through the top surface of the 3D-printed scaffolds, and down the z axis. The outlet fluid did exit from the bottom surface of the 3D-printed scaffolds. As a result the internal fluid was perfusing the whole volume of the 3D-printed scaffolds, thereby creating fluid flow dynamics (fluid velocity, fluid shear stress, and wall shear stress) distribution inside the 3D-printed scaffolds in the perfusion bioreactor.

Computational model

Computational models were implemented using the finite element software COMSOL Multiphysics (v5.2) to simulate fluid flow dynamics inside the 3D-printed scaffolds in a perfusion bioreactor. Structured volume mesh with 317219 elements (tetrahedral elements: 231206, pyramids: 648, triangles: 55696, edge elements: 5448) was used to accurately calculate the fluid flow dynamics inside the scaffolds by the finite element model. The meshed state of the simulation volume of the 3D-printed scaffold geometry was indicated (Fig. 1).

Governing equation

Navier-Stokes equation (momentum (equation 1) and continuity (Equation (2)) was used to model a fully developed laminar fluid flow [31].

$$\rho\frac{\partial u}{\partial t}-\mu\nabla^2u+\rho(u.\nabla)u+\nabla P=F \quad (1)$$

$$\nabla.u=0 \quad (2)$$

Where u, ρ, μ, and p are the fluid velocity field, fluid density, fluid dynamic viscosity, and fluid pressure respectively. Moreover, F indicates forces such as gravity

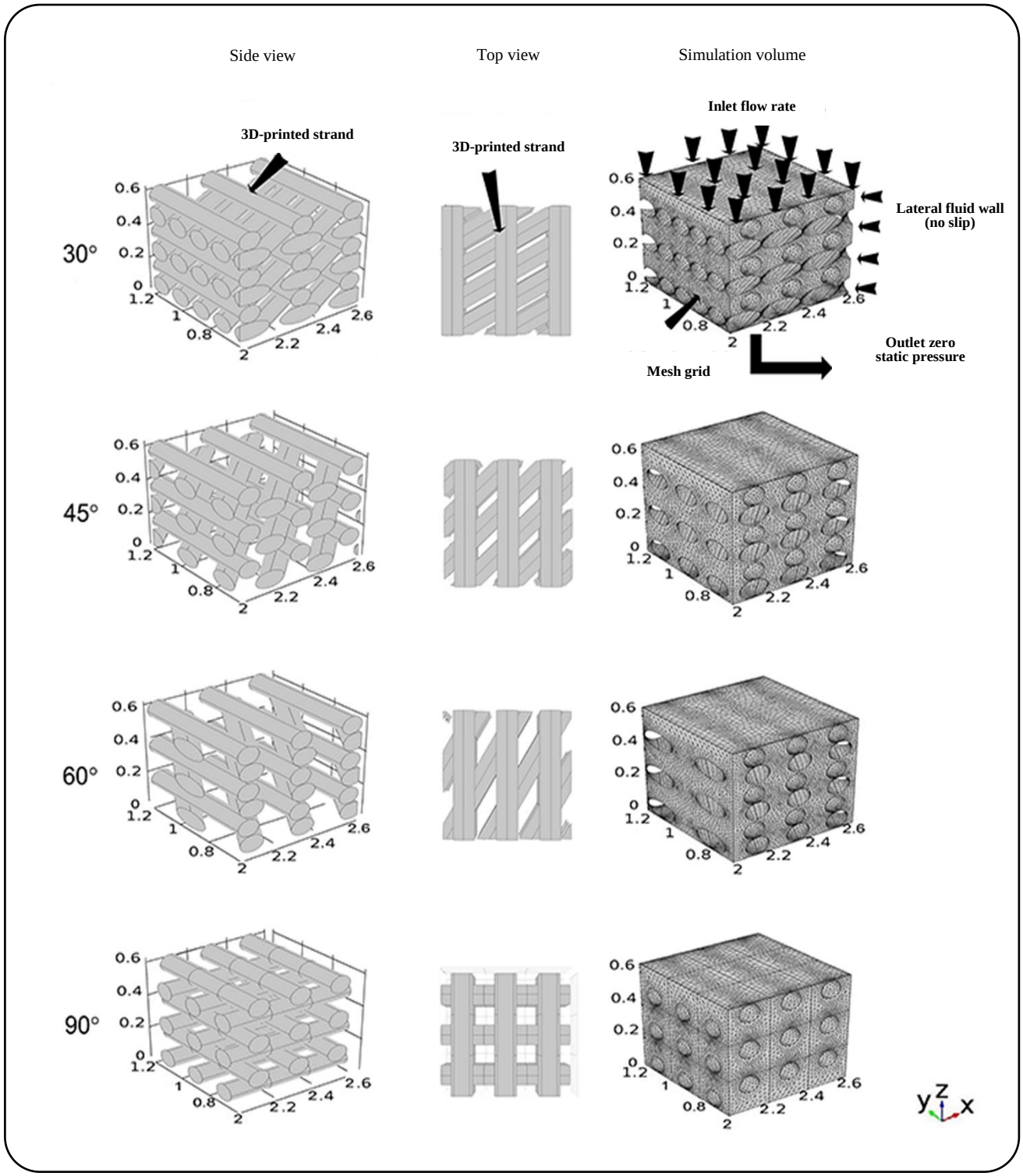

Fig. 1: Schematic illustration of a 3D-printed scaffold containing strands with different angular orientation (30°, 45°, 60°, and 90° between strands in each layer) used to simulate fluid velocity, fluid shear stress, and wall shear stress inside a perfusion bioreactor. Side view of the 3D-printed scaffold containing strands showing the inner surface of the scaffold. Top view of the 3D-printed scaffold containing strands showing strands geometry between each layer inside the scaffold. Simulation volume showed boundary conditions (inlet flow rate, outlet zero static pressure, no wall slip) and mesh grid applied in the numerical method. 3D-printed scaffold length×width×height: 0.6×0.6×0.6 cm; total volume: 216×10^{-3} cm^3; strand diameter: 100 μm.

and centrifugal force; F was set to zero in the present study [31, 32].

Solving the Navier-Stokes equation numerically yielded the fluid velocity field and fluid pressure. From the fluid velocity information, the fluid shear stress (τ) was attained by using the following constitutive relation for a Newtonian fluid:

$$\tau_{ij} = \mu \left(\frac{\partial U_i}{\partial X_j} + \frac{\partial U_j}{\partial X_i} \right) \quad (3)$$

Boundary conditions

In a perfusion bioreactor, the inlet fluid enters the scaffolds homogeneously from the top surface of the 3D-printed scaffolds. A constant flow rate boundary condition was imposed at the inlet section located at the top surface of the scaffolds. The magnitude of the inlet flow rate (0.02, 0.1, and 0.5 mL/min) was chosen based on that in peristaltic pumps (range 0.02 to 1 mL/min) generally used in experimental and simulation studies on perfusion bioreactors [7, 30, 33]. The flow connects with the inside flow of the 3D-printed scaffolds and the outlet fluid, which is located at the bottom surface of the scaffolds, through the open channels between the strands. The lateral fluid walls were treated as closed walls with a no slip condition. The average fluid pressure at the outlet surface of the scaffolds was set to zero (Fig. 1). The fluid flow was considered laminar since the fluid velocity was low (<1200 μm/s) in combination with micro-dimension of channel width (200 μm) inside the 3D-printed scaffolds. The fluid flow was modeled as an incompressible and homogeneous Newtonian fluid with ρ = 1,000 kg/m^3 and dynamic viscosity of 8.9×10^{-4} Pa.s [34].

RESULTS AND DISCUSSION

We employed computational evaluation to assess the distribution and magnitude of fluid velocity, fluid shear stress, and wall shear stress inside 3D-printed scaffolds containing strands with different angular orientation between strands in each layer within a perfusion bioreactor. The simulation volume, boundary conditions, and mesh grids applied to the finite element model are depicted in Fig. 1, where the inlet flow was assumed to enter homogeneously from the top surface to the bottom surface of the scaffolds, and the fluid was assumed to flow inside the scaffolds through open channels between strands. We found that 3D-printed scaffold architecture and inlet flow rate of a perfusion bioreactor dictate fluid velocity, fluid shear stress, wall shear stress distribution and magnitude inside the scaffolds, which is highly relevant since mechanical stimuli affect cells [25, 35].

The fluid velocity corresponding to 0.02, 0.1, and 0.5 mL/min inlet flow rate inside a 3D-printed scaffolds (30°, 45°, 60°, and 90° angular orientation between strands in each layer) within a perfusion bioreactor was evaluated by computational analysis, and illustrated along the yz plane (Fig. 2). The fluid velocity was symmetric about the xz plane, and the magnitude of the fluid velocity was negative since the fluid was flowing down the z axis (Fig. 2). The perfusion bioreactor provided a strong forward flow without reverse flow within the scaffolds. At 0.02 mL/min inlet flow rate at all angular orientations between strands in each layer, the fluid velocity accelerated from -10 to -50 μm/s through the gap between two strands, and the maximum fluid velocity (-50 μm/s) was found between two strands in each layer (Fig. 2). The magnitude of the fluid velocity was low (< -10 μm/s) in the outlet region and wall planes. At 0.1 ml/min inlet flow rate at all angular orientations between strands in each layer, the fluid velocity accelerated from -50 to -250 μm/s through the gap between two strands, with maximum fluid velocity (-250 μm/s) between two strands in each layer. The magnitude of the fluid velocity was low (< -50 μm/s) in the outlet region and wall planes (Fig. 2). At 0.5 ml/min inlet flow rate at all angular orientations between strands in each layer, the fluid velocity accelerated from -250 to -1250 μm/s through the gap between two strands, and maximum fluid velocity (-1250 μm/s) was found between two strands in each layer (Fig. 2). The magnitude of the fluid velocity was low (< -250 μm/s) in the outlet region and wall planes. When the inlet flow rate was increased by 5-fold (from 0.02 to 0.1 mL/min), the fluid velocity also increased by 5-fold within the scaffolds inside the bioreactor. Spatial inhomogeneity and magnitude of the fluid velocity inside the scaffolds decreased by increasing the angular orientation between strands in each layer as well as by decreasing the inlet flow rate. The fluid velocity decreased at the bottom of the 3D-printed scaffolds due to the increase in the available field of the fluid flow. Since fluid has the tendency to flow in the median available fields between the strands inside the scaffolds, and because there was an effect of pressure difference between inlet flow and outlet flow on the fluid flow inside the scaffolds, the exit fluid velocity was higher than the entrance fluid velocity.

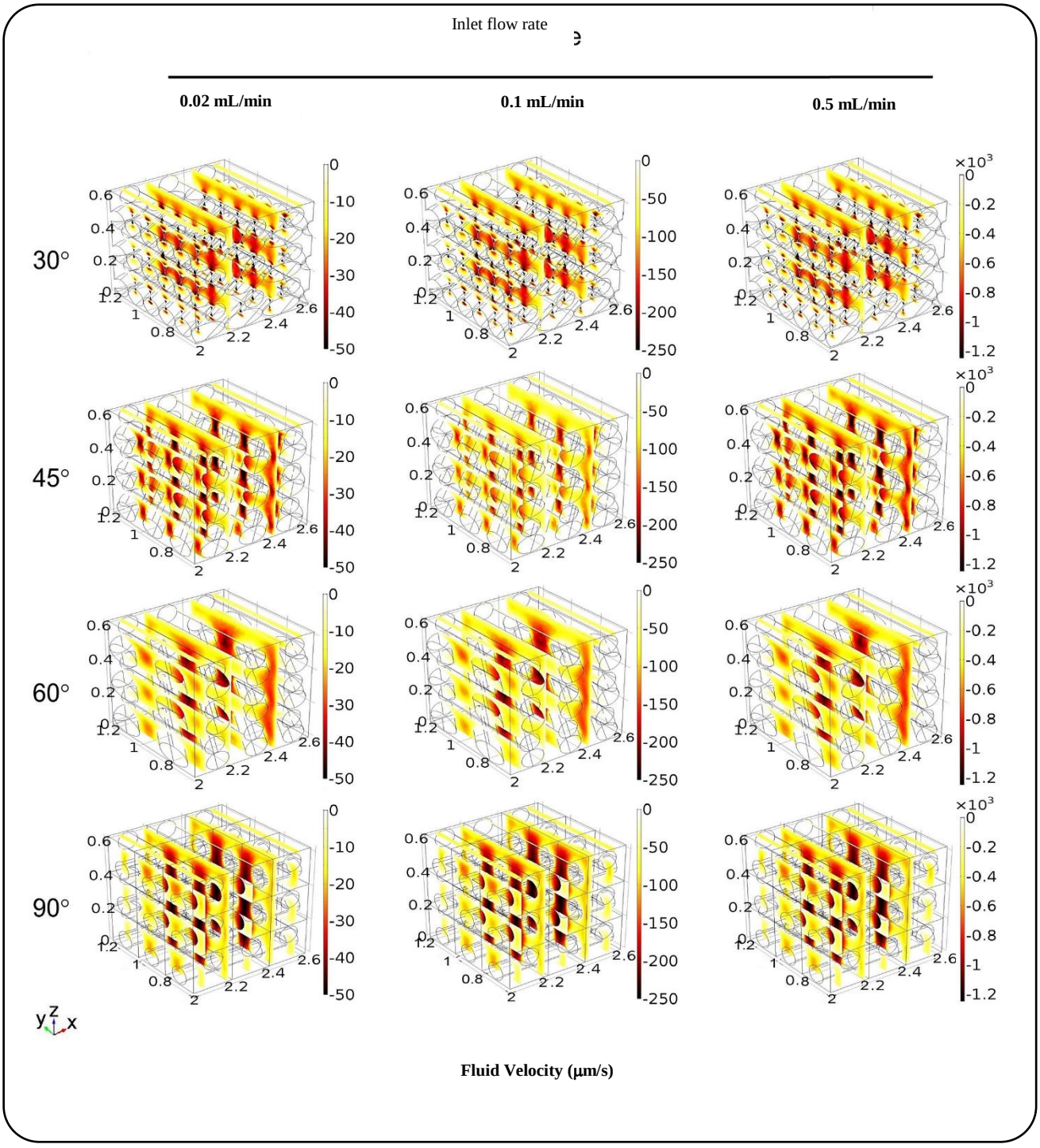

Fig. 2: Effect of angular orientation between 3D-printed strands in each layer at 0.02, 0.1, 0.5 ml/min inlet flow rate of a perfusion bioreactor on the distribution and magnitude of fluid velocity from inlet flow to outlet flow inside the scaffolds. The fluid velocity simulation profiles within the scaffolds with different angular orientation between strands in each layer and different inlet flow rate were calculated. For clarity, five planes were plotted in the x direction. Note, the axes are dissimilar to allow visualization of differences in fluid velocity. Increasing the angular orientation between the strands in each layer (30°, 45°, 60°, and 90°) decreased the magnitude of fluid velocity and the distribution of fluid velocity through the scaffolds. Increasing the inlet flow rate (0.02, 0.1, 0.5 ml/min) increased the magnitude of fluid velocity inside the scaffolds. The x, y, z axes unit; centimeter.

The fluid shear stress corresponding to the 0.2, 0.1, and 0.5 mL/min inlet flow rate inside the 3D-printed scaffolds (with 30°, 45°, 60°, and 90° angular orientation between strands in each layer) within a perfusion bioreactor was simulated, and illustrated along the yz plane (Fig. 3). Since no slip boundary condition was assumed, the gradient of fluid velocity enhanced near the strands surfaces. Thus, maximum fluid shear stress was shown near the strands surfaces. At 0.02 ml/min inlet flow rate at all angular orientations between strands in each layer, the perfusion flow rate produced high shear stress (> 0.25 mPa) through the gap between two strands inside the scaffolds, and maximum fluid shear stress (0.3 mPa) also occurred on the strands surface (Fig. 3). At 0.1 mL/min inlet flow rate at all angular orientations, the perfusion flow rate produced high shear stress (> 1.2 mPa) through the gap between two strands, and maximum fluid shear stress (1.5 mPa) also, occurred on the strands surface (Fig. 3). At 0.5 ml/min inlet flow rate at all angular orientations between strands in each layer, the perfusion flow rate produced high shear stress (> 6 mPa) through the gap between two strands, and maximum fluid shear stress (7 mPa) also occurred on the strands surface (Fig. 3). When the inlet flow rate was increased by 5-fold (from 0.02 to 0.1 mL/min), the fluid shear stress magnitude increased by 5-fold within the scaffolds inside the bioreactor. Spatial inhomogeneity of the fluid shear stress inside the scaffolds decreased by increasing the angular orientation between strands in each layer as well as by decreasing the inlet flow rate. The fluid shear stress magnitude and distribution inside the scaffolds coincided with the fluid velocity gradient. Thus at the entering site the fluid shear stress was high due to a significant change in fluid velocity. Due to increased fluid velocity changes resulting from the passing of the fluid between the strands in each layer inside the scaffolds, the fluid shear stress reached a maximum magnitude inside the 3D-printed scaffolds. Due to slowing down of the fluid velocity changes resulting from the passing of the fluid from each layer of strands inside the scaffolds, the fluid shear stress decreased to a minimum value. The fluid shear stress magnitude decreased at the bottom surface of the scaffolds, as a result of decreasing fluid velocity gradient.

The fluid velocity variation on the surface of the strands inside the scaffolds resulted in wall shear stress, which will affect cells attached to the scaffolds [36, 37]. Variation in angular orientation between strands in each layer inside the 3D-printed scaffolds and in inlet flow rate of the perfusion bioreactor affect the discrete probability distribution of the wall shear stress magnitude (Fig. 4). For all scaffolds with different angular orientation between strands in each layer, the variation of maximum wall shear stress (2 to 0.6 mPa) at 0.02 mL/min inlet flow rate was less than the variation of maximum wall shear stress (from 50 to 15 mPa) at 0.5 mL/min inlet flow rate (Fig. 4). The wall shear stress on the maximum relative area (0.06) was observed at 30° angular orientation, and on the minimum relative area (0.008) at 90° angular orientation. Thus the wall shear stress distribution was more equally at 30° than at 90° angular orientation between strands in each layer of the scaffolds (Fig. 4). The distribution and magnitude of the wall shear stress increased by decreasing the angular orientation between strands in each layer inside the scaffolds, as well as by increasing the inlet flow rate of the perfusion bioreactor.

3D-printed scaffolds with 45°, 60°, and 90°, but not 30° angular orientation between strands in each layer, at inlet flow rates 0.02, 0.1, and 0.5 mL/min showed a wall shear stress of 0.1–10 mPa. Computational fluid dynamics models estimated that a wall shear stress of 0.1–10 mPa on the surface of scaffolds allows bone cell differentiation [38, 39]. In addition, a wall shear stress of 5–15 mPa in a scaffold increases mineralization and accelerates osteogenic differentiation of MSCs [3]. This correlates with our results that >60% of 3D-printed scaffold surface area with 30° angular orientation between strands at all inlet flow rates of the perfusion bioreactor experienced a wall shear stress of 5 to 15 mPa, indicating enhanced osteogenic differentiation of MSCs in these areas. These values of wall shear stress (> 57 mPa) have been shown to be associated with apoptosis [7]. Wall shear stress in the range of 1-33 mPa has been shown to affect cell viability of primary hepatocytes and transformed hepatocyte cell lines [40, 41]. This is in agreement with our findings showing that wall shear stress inside the 3D-printed scaffolds surface area with all angular orientation between strands at 0.1 Lmin and 0.5 mL/min inlet flow rate of the perfusion bioreactor experienced a wall shear stress of 1 to 33 mPa which affects cell viability of primary hepatocytes and transformed hepatocyte cell lines.. Moreover 0.01 mPa wall shear stress significantly alters hepatocyte cytochrome P450 gene expression [42], which agrees with our results that the total surface area of the 3D-printed

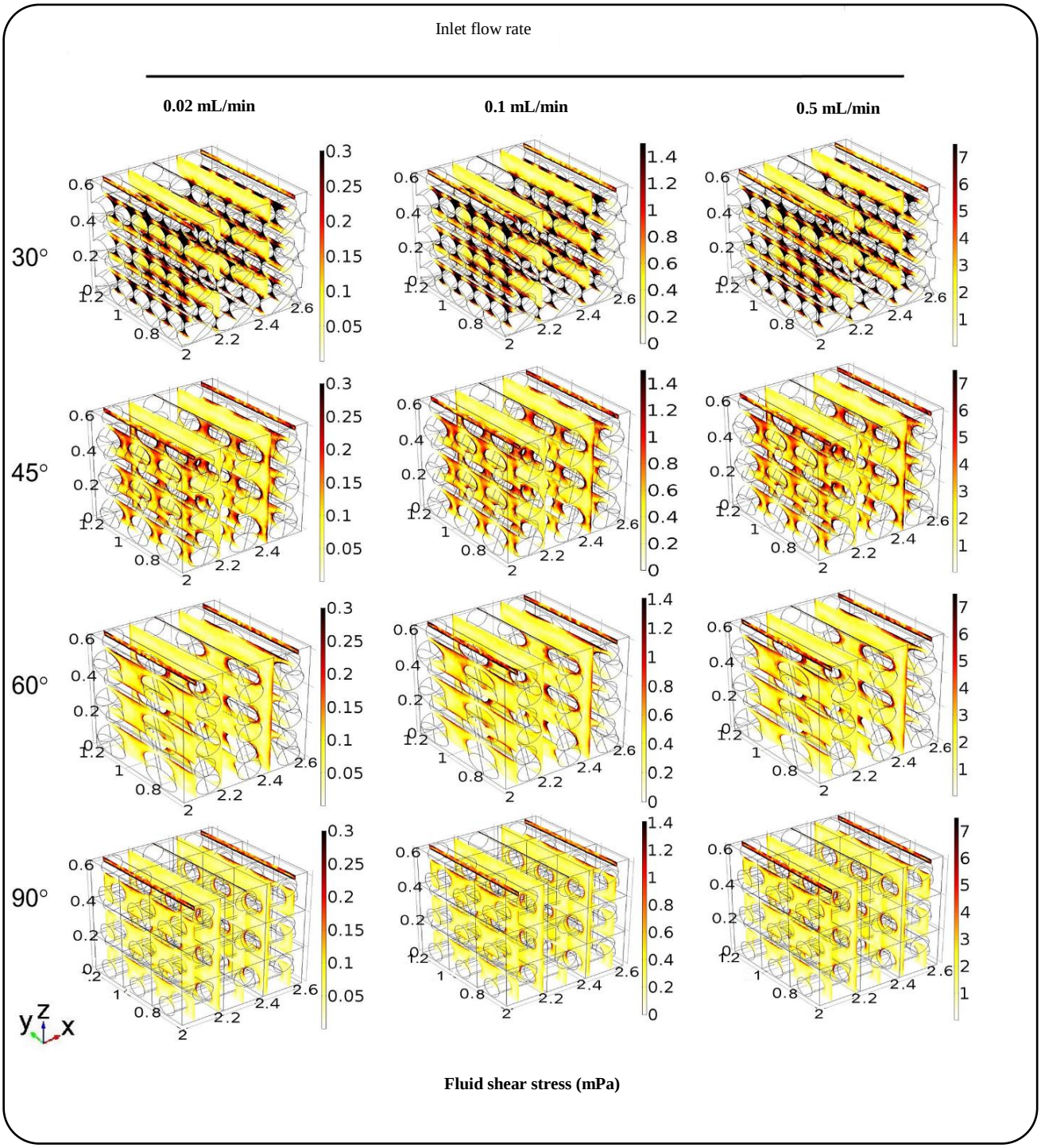

Fig. 3: Effect of angular orientation between 3D-printed strands in each layer at 0.02, 0.1, 0.5 mL/min inlet flow rate of a perfusion bioreactor on the distribution and magnitude of fluid shear stress from inlet flow to outlet flow inside the scaffolds. The fluid shear stress simulation profiles within the scaffolds with different angular orientation between strands in each layer and different inlet flow rate were calculated. For clarity, five planes were plotted in the x direction. Note, the axes are dissimilar to allow visualization of differences in fluid shear stress. Increasing the angular orientation between strands in each layer (30°, 45°, 60°, and 90°) decreased the magnitude of fluid shear stress and the distribution of fluid shear stress through the 3D-printed scaffolds. Increasing the inlet flow rate (0.02, 0.1, 0.5 ml/min) increased the magnitude of fluid shear stress inside the scaffolds. The x, y, z axes unit; centimeter.

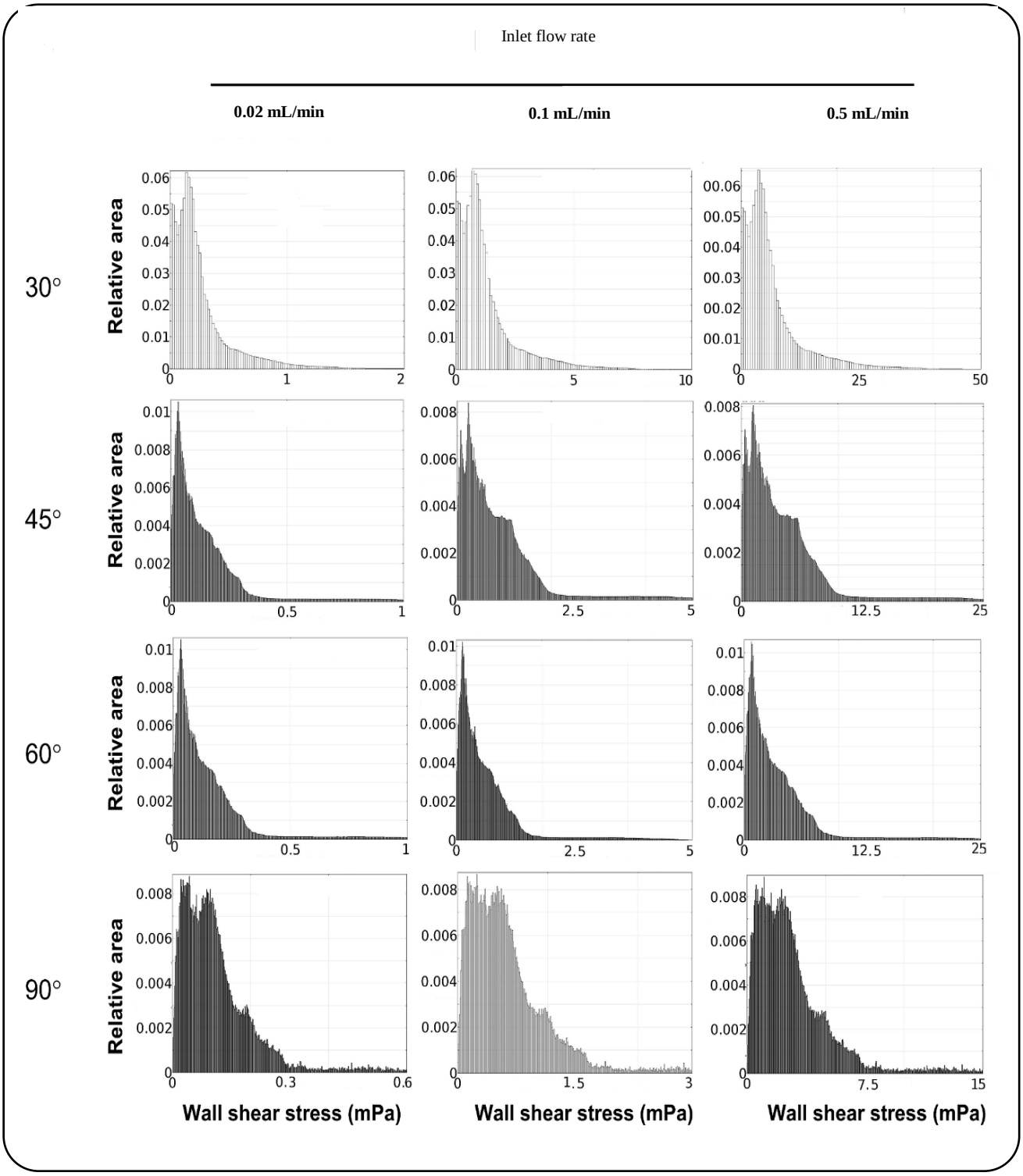

Fig. 4: Angular orientation between strands in each layer of a 3D-printed scaffold and inlet flow rate of a perfusion bioreactor affect the distribution and magnitude of wall shear stress on the strands where cells are attached. Relative area represents the area with a specific wall shear stress, divided by the total area inside the 3D-printed scaffold. The angular orientation between the strands in each layer (30°, 45°, 60°, and 90°) and inlet flow rate (0.02, 0.1, and 0.5 mL/min) of the perfusion bioreactor did affect the magnitude and distribution of wall shear stress inside the scaffold within the perfusion bioreactor.

scaffolds at all inlet flow rates of the perfusion bioreactor experienced a wall shear stress of 0.01 mPa. Our findings suggest that for optimal regulation of the wall shear stress in 3D-printed scaffolds in perfusion bioreactors allowing cell proliferation and/or differentiation, 90° angular orientation between strands in each layer of the scaffold was the best choice due to the lowest wall shear stress dispersion compared to the other angular orientations studied. In addition, the wall shear stress sensitivity at 30° angular orientation between strands was higher than at 45°, 60°, and 90° angular orientation. In other words, a small change in the bioreactor's inlet flow rate will affect the wall shear stress inside the scaffold with 30° angular orientation between strands in each layer more than with 45°, 60°, and 90° angular orientation.

Average fluid velocity, average fluid shear stress, and average wall shear stress inside 3D-printed scaffolds (30°, 45°, 60°, and 90° angular orientation between strands in each layer) within the perfusion bioreactor with 0.02, 0.1, and 0.5 mL/min inlet flow rate related linearly to the inlet flow rate (Fig. 5). At 0.02 ml/min inlet flow rate, strands with 30° angular orientation increased average fluid velocity (1.2-fold), average fluid shear stress (6-fold), and average wall shear stress (1.4-fold) compared to strands at 45°, 60°, and 90° angular orientation. At 0.1 mL/min inlet flow rate, strands at 30° angular orientation increased average fluid velocity (1.3-fold), average fluid shear stress (8-fold), and average wall shear stress (1.8-fold) compared to strands at 45°, 60°, and 90° angular orientation (Fig. 5). At 0.5 ml/min inlet flow rate, strands at 30° angular orientation increased average fluid velocity (1.4-fold), average fluid shear stress (10-fold), and average wall shear stress (2.3-fold) compared to strands at 45°, 60°, and 90° angular orientation. Thus variation of average fluid velocity, average fluid shear stress, and average wall shear stress inside 3D-printed scaffolds with different angular orientation (from 30° to 90°) increased by enhancing the inlet flow rate from 0.02 to 0.5 mL/min. The maximum variation of average fluid velocity, average fluid shear stress, and average wall shear stress at different angular orientation between strands occurred at 0.5 ml/min inlet flow rate of the perfusion bioreactor.

The simulations numerically predicted the wall shear stress at the strands' surface containing attached cells, as a function of several parameters modulating the flow regime and scaffold geometry. We found that the angular

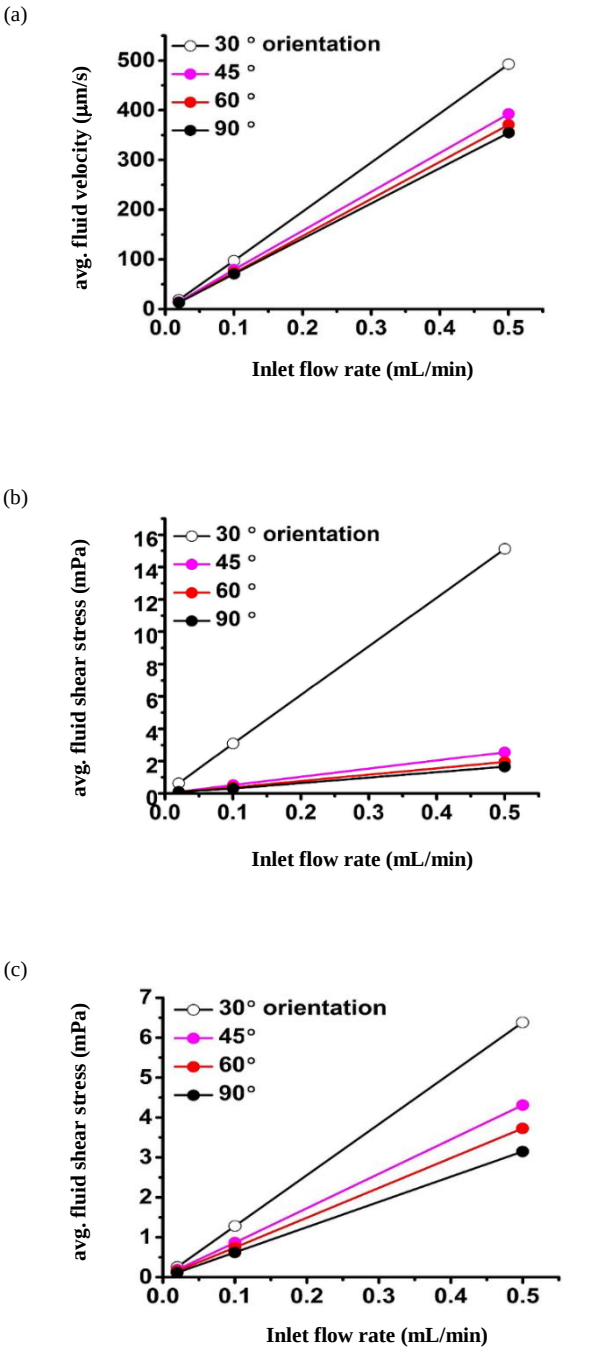

Fig. 5: Angular orientation between strands in each layer of a 3D-printed scaffold and inlet flow rate of a perfusion bioreactor affect average fluid velocity, average fluid shear stress, and average wall shear stress inside the scaffold. The angular orientation between the strands in each layer (30°, 45°, 60°, and 90°) of the scaffold and the inlet flow rate (0.02, 0.1, 0.5 mL/min) did affect (a) average fluid velocity, (b) average fluid shear stress, and (c) average wall shear stress inside the scaffold within the perfusion bioreactor

orientation between strands in each layer inside the scaffold and the inlet flow rate of the perfusion bioreactor are variables strongly influencing the predicted magnitude and distribution of fluid velocity, fluid shear stress, and wall shear stress for a given 3D-printed geometry. Scaffold architecture has been shown to affect fluid flow dynamics within the scaffold [25, 38], which modulates cell deformation. With increments of the inlet flow rate of the perfusion bioreactor, we observed a linear and independent increase in average fluid velocity, average fluid shear stress, and average wall shear stress inside the scaffolds. A similar linear relationship has been computed by others [43, 44]. The fluid velocity, fluid shear stress, and wall shear stress distributions within the scaffold were distributed throughout the scaffolds, since the channels inside the scaffolds were interconnected. The angular orientation between strands in each layer of the scaffold and inlet flow rate of the perfusion bioreactor modulated fluid flow dynamics inside the 3D-printed scaffolds as revealed by using the finite element method.

The presented models lack experimental validation of the estimated shear stress distribution, since it is nearly impossible to quantify fluid flow dynamics (fluid velocity, fluid shear stress, and wall shear stress) distribution inside a scaffold. Measurement of the local velocity field at the scaffold outer walls only is possible (e.g. using laser Doppler velocimetry [45, 46], or particle image velocimetry [47]), but this affects cell growth inside the scaffold. Currently we can only use simulations to predict fluid flow dynamics inside 3D-printed scaffolds.

CONCLUSIONS

We conclude that the angular orientation between strands in each layer inside 3D-printed scaffolds (30°, 45°, 60°, and 90°) in a perfusion bioreactor, and the inlet flow rate of the bioreactor, as controllable parameters, significantly affect the magnitude and distribution of fluid velocity, fluid shear stress, and wall shear stress inside the scaffold. By decreasing the angular orientation between strands in each layer and increasing the inlet flow rate of a perfusion bioreactor, the magnitude and distribution of fluid velocity, fluid shear stress, and wall shear stress inside the scaffold increased. The average fluid velocity, average fluid shear stress, and average wall shear stress inside the scaffold within the bioreactor increased linearly with the inlet flow rate. Our findings provide quantitative insight into the fluid flow dynamics within 3D-printed scaffolds with different geometries containing cells in a perfusion bioreactor, which will have important implications for bone tissue engineering strategies using cells, scaffolds, and bioreactors.

Nomenclatures

u	Flow velocity field, m/s
ρ	Fluid density, kg/m^3
μ	Dynamic viscosity, Pa×s
p	Pressure, Pa
τ	Viscous stress tensor, Pa

Acknowledgment

The authors are thankful to the High Performance Computing Research Center at Amirkabir University of Technology, Tehran, Iran, for providing computational facilities.

Received : Apr. 23, 2019 ; Accepted : Jul. 1, 2019

REFERENCES

[1] Volkmer E., Drosse I., Otto S., Stangelmayer A., Stengele M., Kallukalam B.C., Mutschler W., Schieker M., Hypoxia in Static and Dynamic 3D Culture Systems for Tissue Engineering of Bone, *Tissue Eng. Part A*, **14(8)**: 1331-1340 (2008).

[2] Bjerre L., Bünger C.E., Kassem M., Mygind T., Flow Perfusion Culture of Human Mesenchymal Stem Cells on Silicate-Substituted Tricalcium Phosphate Scaffolds, *Biomaterials*, **29(17)**: 2616-2627 (2008).

[3] Li D., Tang T., Lu J., Dai K., Effects of Flow Shear Stress and Mass Transport on the Construction of a Large-scale Tissue-Engineered Bone in a Perfusion Bioreactor, *Tissue Eng. Part A*, **15(10)**: 2773-2783 (2009).

[4] Cai D.X., Quan Y., He P.J., Tan H.B., Xu Y.Q., Dynamic Perfusion Culture of Human Outgrowth Endothelial Progenitor Cells on Demineralized Bone Matrix *in Vitro*, *Med. Sci. Monit.*, **22**: 4037-4045 (2016).

[5] Kim J., Ma T., Perfusion Regulation of HMSC Microenvironment and Osteogenic Differentiation in 3D Scaffold, *Biotechnol. Bioeng.*, **109(1)**: 252-261 (2012).

[6] Liu C., Abedian R., Meister R., Haasper C., Hurschler C., Krettek C., Von Lewinski G., Jagodzinski M., Influence of Perfusion and Compression on the Proliferation and Differentiation of Bone Mesenchymal Stromal Cells Seeded on Polyurethane Scaffolds, *Biomaterials*, **33(4)**:1052-1064 (2012).

[7] Cartmell S.H., Porter B.D., García A.J., Guldberg, R.E., Effects of Medium Perfusion Rate on Cell-Seeded Three-dimensional Bone Constructs *in Vitro*, *Tissue Eng.*, **9(6)**: 1197-1203 (2003).

[8] Sittichockechaiwut A., Scutt A.M., Ryan A.J., Bonewald, L.F., Reilly G.C., Use of Rapidly Mineralising Osteoblasts and Short Periods of Mechanical Loading to Accelerate Matrix Maturation in 3D Scaffolds, *Bone*, **44(5)**: 822-829 (2009).

[9] Bacabac R.G., Smit T.H., Mullender M.G., Dijcks S.J., Van Loon J.J., Klein-Nulend J., Nitric Oxide Production by Bone Cells is Fluid Shear Stress Rate Dependent, *Biochem. Biophys. Res. Commun.*, **315(4)**: 823-829 (2004).

[10] Klein-Nulend J., Van der Plas A., Semeins C.M., Ajubi N.E., Frangos J.A., Nijweide P.J., Burger E.H., Sensitivity of Osteocytes to Biomechanical Stress *in Vitro*, *FASEB J.*, **9(5)**: 441-445 (1995).

[11] Rubin J., Rubin C., Jacobs C.R., Molecular Pathways Mediating Mechanical Signaling in Bone, *Gene*, **367**:1-16 (2006).

[12] Weinbaum S., Cowin S.C., Zeng Y., A Model for the Excitation of Osteocytes by Mechanical Loading-induced Bone Fluid Shear Stresses, *J. Biomech.*, **27(3)**: 339-360 (1994).

[13] Song M.J., Dean D., Tate M.L.K., Mechanical Modulation of Nascent Stem Cell Lineage Commitment in Tissue Engineering Scaffolds, *Biomaterials*, **34(23)**: 5766-5775 (2013).

[14] Yue D., Zhang M., Lu J., Zhou J., Bai Y., Pan J., The Rate of Fluid Shear Stress is a Potent Regulator for the Differentiation of Mesenchymal Stem Cells, *J. Cell. Physiol.*, (2019).

[15] Papantoniou I., Chai Y.C., Luyten F.P., Schrooten J., Process Quality Engineering for Bioreactor-driven Manufacturing of Tissue-engineered Constructs for Bone Regeneration, *Tissue Eng. Part C Methods*, **19(8)**: 596-609 (2013).

[16] Elashry M.I., Gegnaw S.T., Klymiuk M.C., Wenisch S., Arnhold S., Influence of Mechanical Fluid Shear Stress on the Osteogenic Differentiation Protocols for Equine Adipose Tissue-Derived Mesenchymal Stem Cells, *Acta Histochem.*, **121(3)**: 344-353 (2019).

[17] Li Y., Fang X., Jiang T., Minimally Traumatic Alveolar Ridge Augmentation with a Tunnel Injectable Thermo-sensitive Alginate Scaffold, *J. Appl. Oral. Sci.*, **23(2)**: 215-223 (2015).

[18] Zhu X., Zhong T., Huang R., Wan A., Preparation of Hydrophilic Poly(lactic acid) Tissue Engineering Scaffold *via* (PLA)-(PLA-b-PEG)-(PEG) Solution Casting and Thermal-induced Surface Structural Transformation, *J. Biomater. Sci. Polym. Ed.*, **26(17)**: 1286-1296 (2015).

[19] Liu S., He Z., Xu G., Xiao X., Fabrication of Polycaprolactone Nanofibrous Scaffolds by Facile Phase Separation Approach, *Mater. Sci. Eng. C Mater. Biol. Appl.*, **44**: 201-208 (2014).

[20] Haugh M.G., Murphy C.M., O'Brien F.J., Novel Freeze-drying Methods to Produce a Range of Collagen-glycosaminoglycan Scaffolds with Tailored Mean Pore Sizes, *Tissue Eng. Part C Methods*, **16(5)**:887-94 (2010).

[21] Hollister S.J., Porous Scaffold Design for Tissue Engineering, *Nat. Mater.*, **4(7)**:518-524 (2005).

[22] Stevens B., Yang Y., Mohandas A., Stucker B., Nguyen K.T., A Review of Materials, Fabrication Methods, and Strategies Used to Enhance Bone Regeneration in Engineered Bone Tissues, *J. Biomed. Mater. Res. B Appl. Biomater.*, **85(2)**:573-582 (2008).

[23] Wu C., Luo Y., Cuniberti G., Xiao Y., Gelinsky M., Three-dimensional Printing of Hierarchical and Tough Mesoporous Bioactive Glass Scaffolds with a Controllable Pore Architecture, Excellent Mechanical Strength and Mineralization Ability, *Acta Biomater.*, **7(6)**: 2644-2650 (2011).

[24] Pfister A., Landers R., Laib A., Hübner U., Schmelzeisen R., Mülhaupt R., Biofunctional Rapid Prototyping for Tissue-engineering Applications: 3D Bioplotting Versus 3D Printing, *J. Polym. Sci. Pol. Chem.*, **42(3)**: 624-638 (2004).

[25] Bartnikowski M., Klein T.J., Melchels F.P., Woodruff M.A., Effects of Scaffold Architecture on Mechanical Characteristics and Osteoblast Response to Static and Perfusion Bioreactor Cultures, *Biotechnol. Bioeng.*, **111(7)**: 1440-1451 (2014).

[26] Hossain M.S., Boergstrom D.J., Chen X.B., Prediction of Cell Growth Rate over Scaffold Strands inside a Perfusion Bioreactor, *Biomech. Model. Mechanobiol.*, **14(2)**: 333-44 (2015).

[27] Lesman A., Blinder Y., Levenberg S., Modeling of Flow-induced Shear Stress Applied on 3D Cellular Scaffolds: Implications for Vascular Tissue Engineering, *Biotechnol. Bioeng.*, **105(3)**:645-54 (2010).

[28] Hutmacher D.W., Singh H., Computational Fluid Dynamics for Improved Bioreactor Design and 3D Culture, *Trends Biotechnol.*, **26(4)**: 166-72 (2008).

[29] Boschetti F., Raimondi M.T., Migliavacca F., Dubini G., Prediction of the Micro-fluid Dynamic Environment Imposed to Three-dimensional Engineered Cell Systems in Bioreactors, *J. Biomech.*, **39(3)**: 418-25 (2006).

[30] Maes F., Claessens T., Moesen M., Van Oosterwyck H., Van Ransbeeck P., Verdonck P., Computational Models for Wall Shear Stress Estimation in Scaffolds: a Comparative Study of Two Complete Geometries, *J. Biomech.*, **45(9)**: 1586-92 (2012).

[31] Vossenberg P., Higuera G.A., Van Straten G., Van Blitterswijk C.A., Van Boxtel A.J.B., Darcian Permeability Constant as Indicator for Shear Stresses in Regular Scaffold Systems for Tissue Engineering, *Biomech. Model. Mechanobiol.*, **8(6)**: 499-507 (2009).

[32] Xue X., Patel M.K., Kersaudy-Kerhoas M., Desmulliez M.P., Bailey C., Topham D., Analysis of Fluid Separation in Microfluidic T-channels, *Appl. Math. Model.*, **36(2)**: 743-755 (2012).

[33] McCoy R.J., Jungreuthmayer C., O'Brien F.J., Influence of Flow Rate and Scaffold Pore Size on Cell Behavior During Mechanical Stimulation in a Flow Perfusion Bioreactor, *Biotechnol. Bioeng.*, **109(6)**: 1583-9154 (2012).

[34] Campos Marin A., Lacroix D., The Inter-sample Structural Variability of Regular Tissue-engineered Scaffolds Significantly Affects the Micromechanical Local Cell Environment, *Interface Focus*, **5(2)**: 20140097 (2015).

[35] Bakker A.D., Gakes T., Hogervorst J.M., De Wit G.M., Klein-Nulend J., Jaspers R.T., Mechanical Stimulation and IGF-1 Enhance mRNA Translation Rate in Osteoblasts via Activation of the AKT-mTOR Pathway, *J. Cell. Physiol.*, **231(6)**:1283-1290 (2016).

[36] Knippenberg M., Helder M.N., Zandieh Doulabi B., Semeins C.M., Wuisman P.I., Klein-Nulend J., Adipose Tissue-derived Mesenchymal Stem Cells Acquire Bone Cell-like Responsiveness to Fluid Shear Stress on Osteogenic Stimulation, *Tissue Eng.*, **11(11-12)**:1780-1788 (2005).

[37] Wittkowske C., Reilly G.C., Lacroix D., Perrault C.M., *In Vitro* Bone Cell Models: Impact of Fluid Shear Stress on Bone Formation, *Front. Bioeng. Biotechnol*., **4**:87 (2016).

[38] Olivares A.L., Marsal È., Planell J.A., Lacroix D., Finite Element Study of Scaffold Architecture Design and Culture Conditions for Tissue Engineering, *Biomaterials*, **30(30)**:6142-6149 (2009).

[39] Prendergast P.J., Huiskes R., Soballe K., Biophysical Stimuli on Cells During Tissue Differentiation at Implant Interfaces, *J. Biomech.*, **30(6)**:539-548 (1997).

[40] Park J., Li Y., Berthiaume F., Toner M., Yarmush M.L., Tilles A.W., Radial Flow Hepatocyte Bioreactor Using Stacked Microfabricated Grooved Substrates, *Biotechnol. Bioeng.*, **99(2)**: 455-467 (2008).

[41] Tilles A.W., Baskaran H., Roy P., Yarmush M.L., Toner M., Effects of Oxygenation and Flow on the Viability and Function of Rat Hepatocytes Cocultured in a Microchannel Flat-plate Bioreactor, *Biotechnol. Bioeng.*, **73(5)**: 379-389 (2001).

[42] Vinci B., Duret C., Klieber S., Gerbal-Chaloin S., Sa-Cunha A., Laporte S., Suc B., Maurel P., Ahluwalia A., Daujat-Chavanieu M., Modular Bioreactor for Primary Human Hepatocyte Culture: Medium Flow Stimulates Expression and Activity of Detoxification Genes, *Biotechnol. J.*, **6(5)**: 554-564 (2011).

[43] Sandino C., Planell J.A., Lacroix D., A Finite Element Study of Mechanical Stimuli in Scaffolds for Bone Tissue Engineering, *J. Biomech.*, **41(5)**: 1005-1014 (2008).

[44] Yan X., Chen X., Bergstrom D.J., Modeling of the Flow within Scaffolds in Perfusion Bioreactors, *Am. J. Biomed. Eng.*, **1(2)**:72-77 (2011).

[45] Hollnagel D.I., Summers P.E., Poulikakos D., Kollias S.S., Comparative Velocity Investigations in Cerebral Arteries and Aneurysms: 3D Phase-contrast MR Angiography, Laser Doppler Velocimetry and Computational Fluid Dynamics, *NMR Biomed.*, **22(8)**:795-808 (2009).

[46] Yap C.H., Saikrishnan N., Yoganathan A.P., Experimental Measurement of Dynamic Fluid Shear Stress on the Ventricular Surface of the Aortic Valve Leaflet, *Biomech. Model. Mechanobiol.*, **11(1-2)**: 231-244 (2012).

[47] Roloff C., Berg P., Redel T., Janiga G., Thévenin D., Tomographic Particle Image Velocimetry for the Validation of Hemodynamic Simulations in an Intracranial Aneurysm, *Conf. Proc. IEEE Eng. Med. Biol. Soc.*, **2017**: 1340-1343 (2017).